Sacred Heart UNIVERSITY

Sacred Heart University
DigitalCommons@SHU

Biology Faculty Publications | Biology

1-2015

Evaluation of the Developmental Toxicity of Lead in the Danio rerio Body

Nicole M. Roy
Sacred Heart University, royn@sacredheart.edu

Sarah DeWolf
Sacred Heart University, dewolfs@sacredheart.edu

Bruno Carneiro
Sacred Heart University, carneirob@sacredheart.edu

Follow this and additional works at: https://digitalcommons.sacredheart.edu/bio_fac


Part of the Cell and Developmental Biology Commons, Laboratory and Basic Science Research Commons, and the Neuroscience and Neurobiology Commons

Recommended Citation

Roy, N.M., DeWolf, S. & Carneiro, B. (2015). Evaluation of the developmental toxicity of lead in the Danio rerio body. *Aquatic Toxicology, 158*,138-148. doi: 10.1016/j.aquatox.2014.10.026

This Peer-Reviewed Article is brought to you for free and open access by the Biology at DigitalCommons@SHU. It has been accepted for inclusion in Biology Faculty Publications by an authorized administrator of DigitalCommons@SHU. For more information, please contact ferribyp@sacredheart.edu, lysobeyb@sacredheart.edu.

Accepted Manuscript

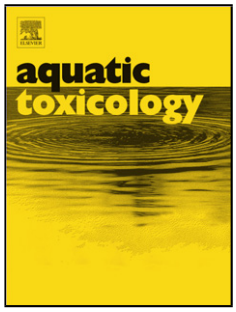

Title: Evaluation of the Developmental Toxicity of Lead in the *Danio rerio* Body

Author: Nicole M. Roy Sarah DeWolf Bruno Carneiro

PII: S0166-445X(14)00332-4
DOI: http://dx.doi.org/doi:10.1016/j.aquatox.2014.10.026
Reference: AQTOX 3968

To appear in: *Aquatic Toxicology*

Received date: 3-9-2014
Revised date: 30-10-2014
Accepted date: 31-10-2014

Please cite this article as: Roy, N.M., DeWolf, S., Carneiro, B.,Evaluation of the Developmental Toxicity of Lead in the *Danio rerio* Body, *Aquatic Toxicology* (2014), http://dx.doi.org/10.1016/j.aquatox.2014.10.026

This is a PDF file of an unedited manuscript that has been accepted for publication. As a service to our customers we are providing this early version of the manuscript. The manuscript will undergo copyediting, typesetting, and review of the resulting proof before it is published in its final form. Please note that during the production process errors may be discovered which could affect the content, and all legal disclaimers that apply to the journal pertain.

ACCEPTED MANUSCRIPT

Highlights

- Lead treatment induces curvature of the spine
- We demonstrate changes in somites including decreased size, altered gene expression and altered muscle myofibrils
- We demonstrate alterations in body vasculature and motor neuron development as well as increased apoptosis

Accepted Manuscript

ACCEPTED MANUSCRIPT

Evaluation of the Developmental Toxicity of Lead in the *Danio rerio* Body

Nicole M. Roy*, Sarah DeWolf*, and Bruno Carneiro*

* Department of Biology, Sacred Heart University, Fairfield CT

Corresponding Author

Nicole M. Roy

Phone: 203-365-4772

Fax: 203-365-4785

E-mail: royn@sacredheart.edu

Mailing Address: Sacred Heart University, Biology Department

5151 Park Ave, Fairfield, CT 06825

Accepted Manuscript

ACCEPTED MANUSCRIPT

Abstract

Lead has been utilized throughout history and is widely distributed and mobilized globally. Although lead in the environment has been somewhat mitigated, the nature of lead and its extensive uses in the past prohibit it from being completely absent from our environment and exposure to lead is still a public health concern. Most studies regarding lead toxicity have focused on the brain. However, little is found in the literature on the effects of lead in other tissues. Here, we utilize the zebrafish model system to investigate effects of lead exposure during early developmental time windows at 24, 48 and 72 hours post fertilization in the body. We analyze whole body, notochord and somatic muscle changes, vascular changes of the body, as well as motor neuron alterations. We find lead exposure induces a curved body phenotype with concomitant changes in somite length, decreased notochord staining and abnormal muscle staining using live and *in situ* approaches. Furthermore, altered vasculature within the somatic regions, loss and/or alternations of motor neuron extension both dorsally and ventrally from the spinal cord, loss of Rohon-Beard sensory neurons, and increased areas of apoptosis were found. We conclude that lead is developmentally toxic to other areas of the developing embryo, not just the brain.

Keywords: Zebrafish, Development, Lead, Vasculature, Notochord, Neurons

Accepted Manuscript

ACCEPTED MANUSCRIPT

1. Introduction

Lead has been mined and used for over 6000 years, spiking during Roman times and the Industrial Revolution (Hernberg, 2000; Philp, 2001). During the past 100 years, lead was exclusively used in paints, canning, toy manufacturing, pesticides, lead shot, and as a gas additive (Philp, 2001; Roy et al., 2014). In the United States, use of lead in many products has been banned since the 1970's, however, lead continues to contaminate our environment and is found in dust, street dirt, soil, water and food (Tong et al., 2000). Current sources of lead exposure include past emissions of leaded gasoline accumulating in soil, abandoned industrial sites, smelting operations, older homes with leaded paint and lead pipes, as well as imported toys (Philp, 2001; Tong et al., 2000). Furthermore, a number of home hobbies can contribute to lead contamination including pottery and stained glass. Because lead was utilized globally and in such vast quantities, mitigating all the lead in our environment is impossible. Chronic exposure to low levels of lead is a common health issue and acute lead poisoning can still occur, especially among socioeconomically disadvantaged groups and in developing countries lacking policies and environmental regulations (Tong et al., 2000).

The zebrafish model has become particularly popular in the laboratory setting given its genetic and embryological similarities to higher order vertebrates including humans (Grunwald and Eisen, 2002). Zebrafish share a high degree of homology with the human genome (Dai et al., 2014; Howe et al., 2013) and thus, modeling of human diseases in zebrafish is now commonplace. From a toxicological perspective, zebrafish are particularly useful as their development is very well characterized (Hill et al., 2005; Kimmel et al., 1995) and all stages of toxicological assessment can be made *ex utero.* Of particular toxicological significance to the

Accepted Manuscript

ACCEPTED MANUSCRIPT

model, they develop organs specific to toxin conversion, like the liver, very early in their development. They also share the same liver metabolic pathways and cytochrome P450 (CYP) genes, most of which are direct orthologs of human CYPs (Goldstone et al., 2010; Padilla et al., 2012; Tao and Peng, 2009). Thus, the zebrafish can provide information that could not be gathered from other models and knowledge of the mechanisms of developmental toxicity is scarce (Teraoka et al., 2003). Since the zebrafish genome has been sequenced, fluorescent transgenic zebrafish are relatively easy to construct and are visualized well in the optically transparent zebrafish embryo. As zebrafish rapidly mature, transgenerational effects of toxin exposure can be assessed (Hill et al., 2005). From an eco-toxicological perspective, zebrafish have been extensively used to study heavy metals, endocrine disrupting chemicals, and persistent organic pollutants (Dai et al., 2014).

Traditional approaches to toxicology include testing on common laboratory species like rat or rabbit, but this approach is time consuming and expensive. Given the number of chemicals entering the market, the need for high throughput assays is significant. The goal of the United States Environmental Protection Agency (EPA) ToxCast^{TM} program is to develop cost-effective approaches to rapidly screen and prioritize chemicals that would require further toxicological testing. High throughput testing has mainly involved *in vitro* assays and *in silico* modeling (Padilla et al., 2012). However, in recent years, numerous labs have correlated zebrafish developmental toxicity with mammalian developmental toxicity validating the model (Busquet et al., 2008; Padilla et al., 2012; Selderslaghs et al., 2009) and thus, the EPA has recently launched a new toxicological initiative within the umbrella of the ToxCast^{TM} program to utilize zebrafish developmental toxicity to model human health. Two approaches can be taken to study developmental toxicity: a low dose chronic exposure or a short high dose exposure. The

ACCEPTED MANUSCRIPT

ToxCast™ program utilizes the latter approach and treats embryos at early developmental time points with toxic chemicals at relatively high doses to investigate overt phenotypes and other organismal toxicity (Padilla et al., 2012) for predictive modeling of human developmental toxicity. Although there is a wealth of knowledge on low dose chronic exposure to lead in children and its association with reduced IQ (Intelligence Quotient), ADHD (Attention Deficit Hyperactivity Disorder), and decreased cognitive abilities and hyperactivity (Lidsky and Schneider, 2003; Needleman, 2004; Philp, 2001; Tong et al., 2000), there are few publications in the literature on short, high dose exposures. Here, we have sought to model the EPA ToxCast™ approach to investigate a shorter high dose exposure and its effect on the developing body. A high dose, short exposure of lead in zebrafish was investigated by Dou and Zhang, (2011), who found decreased *gfap* and *huC* gene expression in the diencephalon indicating neurogenesis was significantly compromised by lead during embryonic development (Dou and Zhang, 2011). However, they noted only slight changes in two other genes required for neurogenesis, *ngn1* and *crestin. Neurogenin1* is expressed in the central nervous system (CNS), otic and epibranchial placodes and *crestin* in cranial and trunk neural crest cells. However, their investigation on the effects of lead did not proceed past the 24hr time point (Dou and Zhang, 2011). Springboarding off of their work and utilizing the same lead dose, we have also found structural abnormalities in the hindbrain including alterations in branchiomotor neuron development and migration. Altered neural vasculature and increased neural apoptosis were also noted (Roy et al., 2014). Here, we hypothesize that lead will also demonstrate developmental toxicity to other areas in addition to the brain and we investigate the effects of lead looking at live gross body phenotypes, notochord and muscle changes using an *in situ* and immunohistological approach and spinal neuron changes using a transgenic approach. We find

ACCEPTED MANUSCRIPT

lead exposure induces a curved body phenotype with concomitant changes in somite length, decreased notochord staining and altered muscle staining using live and *in situ* approaches. Additionally, altered vasculature within the somatic regions, loss and/or alterations of motor neurons extending dorsally and ventrally from the spinal cord, loss of Rohon-Beard sensory neurons, and increased areas of apoptosis were found. We conclude that lead is developmentally toxic to other areas of the developing embryo, not just the brain.

2. Materials and Methods

2.1 Zebrafish Breeding and Embryo Maintenance

Adult zebrafish were housed in the Sacred Heart University Animal Facility in a standard zebrafish module (ZMOD (zebrafish module), Aquatic Habitats, Inc). Adults were fed once daily with a combination of brine shrimp and supplemental TetraMin® Flake food. A 10% water change was performed and water quality was monitored daily in accordance with IACUC (Institutional Animal Care and Use Committees) regulations. Ammonia levels were kept below 0.5ppm, nitrate levels below 80ppm, nitrite levels below 1ppm and the pH was kept between 6.5-7.5. The adults were maintained on a standard 14:10 hour light:dark wake to sleep cycle. Two adult male and female pairs were placed in standard breeding boxes for mating purposes (Westerfield, 1993). Embryos were collected the following morning and placed in 30% Danieau Buffer (Westerfield, 1993) prior to lead treatment. Transgenic *fli-1 gfp* zebrafish were a generous gift from the Lawson Lab (University of Massachusetts Medical Center). Transgenic *neurogenin1 gfp* and *islet-1 gfp* zebrafish were generous donations from the Linney Lab (Duke

ACCEPTED MANUSCRIPT

University Medical Center). All embryos were staged according to Kimmel (Kimmel et al., 1995).

2.2 Lead Acetate and Exposure Protocol

Lead acetate was obtained from Sigma-Aldrich Chemical Company. Solid lead powder was dissolved in 30% Danieau Buffer to a final concentration of 0.2mM. Embryos were transferred to the control (30% Danieau Buffer) or lead solution (0.2mM) at 6 hour post fertilization (hpf) and treated continuously until 24, 48 and 72hpf when they were released from the lead treatment to control water. As we wished to investigate the effect of lead on body development, treatments commenced at 6hpf to coincide with the onset of gastrulation. After the treatment window ended (after 24, 48 or 72hpf), embryos were transferred to control water for safety purposes during imaging. Treatments were performed in standard Petri dishes at 28.5º C as previously described (Roy et al., 2014). Lead solution was changed daily and a maximum of 50 embryos were placed in each dish.

2.3 Determination of Dose

An LD_{50} was previously determined and the rationale for using the 0.2 mM dose was previously described (Roy et al., 2014). Embryonic survivability at the dose was also previously described (Roy et al., 2014). The 0.2 mM dose was also previously used to investigate the effect of lead on swimming patterns and to assess larval escape responses (Dou and Zhang, 2011).

2.4 Imaging and Microscopy (transgenic and non-transgenic embryos)

Live images were obtained using a Leica dissection microscope attached to a Nikon Digital Sight DS-2Mv digital camera utilizing QCapture Software. Transgenic green fluorescent images were obtained with a Nikon Eclipse E400 fluorescent microscope attached to a Retiga cooled CCD

Accepted Manuscript

ACCEPTED MANUSCRIPT

(charge-coupled device) camera using QCapture Software. Embryos were sedated in tricaine methanesulfonate (MS-222) (Westerfield, 1993) to inhibit movement during microscopy. Embryos were placed in a depression slide in 3% methylcellulose for positioning purposes (Roy et al., 2014). In some cases (Figure 5, G,I and Figure 6, I), embryos were too curved to obtain in-focus whole body images and were hand manipulated into a straighter position with forceps in 1% agar for imaging.

2.5 Statistics

The experiment was run as three independent trials. For each trial, a total of 10 embryos in the control and lead treatment were imaged and measured at 24, 48 or 72hpf. Thus, the total n for control and lead treatment at the three time points tested was 30. Embryos were chosen at random from the treatment dishes. Measurements of the somites were performed in Photoshop using the ruler function with pre-set measurements of length. The PASW (Predictive Analytics Software) statistics program was utilized. A Shapiro-Wilk normality test was performed prior conducting a 2-way ANOVA with factor of time (24, 48, 72hpf) and treatment (control or lead). A lead treatment *p-value* less than 0.05 is indicated with asterisks.

2.6 Whole mount in situ hybridizations and immunohistochemistry

Protocols for *in situ* hybridization were following according to Sagerström et. al (Sagerstrom et al., 1996). The *ntl* probe was a generous gift from the Sagerström Lab (University of Massachusetts Medical Center, Worcester, MA). The *ntl* probe was utilized as it is a common marker for the notochord (Schulte-Merker et al., 1994; Yamada et al., 1991). The probe was a Digoxigenin (DIG) labeled (Roche LifeScience, 11209256910) antisense RNA probe transcribed using the T7 *in vitro* transcription kit (Promega P1450). The hybridized probes were visualized

ACCEPTED MANUSCRIPT

in blue color using an anti-DIG antibody (Roche LifeScience, 11093274910)

15016	-1	10001	AjaxOrderItemDis	InvalidInputError\	12752
1			-1,-2,-3,-4,-5,-6,-	0	Y
true					

bound to nitroblue tetrazolium and bromo-4-chloro-indolyl phosphate (NBT/BCIP, Promega S3771).

Whole mount immunohistochemistries were performed as previously described (Barresi et al., 2001; Devoto et al., 1996). An F59 antibody specific for myosin heavy chain was obtained from Developmental Studies Hybridoma Bank at the University of Iowa. A 1:5 dilution of supernatant F59 antibody was utilized. FITC-labeled goat anti-mouse secondary antibody (Santa Cruz Biotechnology) was utilized at a 1:200 dilution. Embryos were imaged as described (Roy et al., 2014).

2.7 Apoptotic Staining

Embryos at 24, 48 and 72hpf were treated with Acridine Orange (Sigma-Aldrich Chemical Company, A6014). A stock solution was prepared by dissolving 1mg of Acridine Orange powder into 1ml of distilled water. Embryos were treated with a diluted stock in 30% Danieau Buffer at a concentration of 1µg/ml in Petri dishes for 1-2 hours in the dark. After incubation, embryos were washed extensively in 30% Danieau Buffer and imaged under the fluorescent microscope using the FITC (Fluorescein Isothiocyanate) filter using sedation and imaging procedures are described above.

3. Results and Discussion

Accepted Manuscript

ACCEPTED MANUSCRIPT

Lead is ubiquitous in our environment and exposure to and uptake of lead remains a serious health issue globally. The neurotoxic effects of lead exposure in young children has been documented and linked to a number of behavioral abnormalities and learning disabilities (Dapul and Laraque, 2014; Needleman, 2004). However, most studies investigating lead focus on the brain and there is little in the literature on other toxic effects of lead to the developing embryo. In this study, we focused on development of the body including somitic development, vascularization of the body, motor neuron development and innervation of the somitic tissue during development in the presence of lead.

3.1 Live body measurements

To investigate if lead has other effects on the body beside the brain, we performed a time course of lead exposure and analyzed somite development. Measuring the whole body along the straight A-P axis became problematic at the later time point (72hpf) due to spinal kyphosis. Furthermore, brain ventricle measurements and decreased ventricle lengths have already been noted (Roy et al., 2014). Thus, we measured the length of six somites above the yolk sac extension for standardization. More posterior somites near the tail are more constricted and smaller even in normal development. Somites above the yolk sac extension have reached their consistent and reproducible size at each developmental time point and provide a means to compare lead treated embryos to controls.

Live imaging of the development of embryos in lead solution at 24, 48 and 72hpf was performed to investigate changes in body and somite morphology. No change in general gross morphology was seen between control and lead treatments at the 24hr and 48hr time points (Figure 1, A-H). Somite boundaries in the body and the notochord were clearly defined (Figure 1, B,D,F,H) and no body curving was seen. However, by 48hpf, the lead treated embryos do

Accepted Manuscript

ACCEPTED MANUSCRIPT

demonstrate slightly less optical clarity in the notochord and somites (Figure 1 H). By the 72hr time point, curvature of the spine in lead treatments was seen (Figure 1, I,K) and somites became less clear compared to controls (Figure 1, J,L). Curvature of the spine with lead treatments has also been noted by others (Dou and Zhang, 2011). The notochord also became less optically clear, although the structure was apparent. To assess if lead had any effect on somatic growth, six somites running along the length of the yolk sac extension were measured. The yolk sac extends during the segmentation stage during embryonic development and is well characterized and highly visible, providing a geographical landmark (Kimmel et al., 1995; Virta and Cooper, 2011). A 2-way ANOVA detected a change in the length of the somites over time ($p=<0.001$) consistent with embryonic growth. The 2-way ANOVA showed a significant effect of lead treatment in the somites ($p=<0.001$) and there was a significant interaction between time and lead treatment ($p=<0.001$). It appears that lead had the greatest effect after 72hpf (Figure 2). Thus, somite length decreases due to lead exposure.

3.2 In situ hybridization and immunohistochemistry

As we detected decreased optical clarity in the notochord and somites at 48hpf, and evident changes in somite boundaries and optical clarity by 72hpf, we sought to investigate changes in these structures utilizing a common marker gene for the notochord, *ntl* (Schulte-Merker et al., 1994; Yamada et al., 1991) via *in situ* hybridization and a common muscle myofibril marker F59 via immunohistochemistry. At 24hpf, *ntl* expression in control and lead treated embryos was apparent and strong along the length of the anterioposterior (A-P) body axis (Figure 3, A,B). By 48hpf, *ntl* expression in lead treated embryos decreased with areas of stronger expression in the posterior spine and areas of weaker expression in the anterior spinal

ACCEPTED MANUSCRIPT

region (Figure 3, C,D). By 72hpf, *ntl* expression in lead treated embryos was weak throughout the A-P axis of the notochord (Figure 3, E,F) (Table 1).

At 24 and 48hpf, F59 antibody staining was apparent within the somites in the classic chevron shaped pattern and the linear myofibrils can clearly be seen (Figure 3, G-J). By 72hpf, in lead treated embryos, the linear myofibril expression pattern in the chevron shape became altered (Figure 3, K-N). The somite boundaries can be seen, although they are less linear and clear, as seen in live images in Figure 1, L. Gaps in the myofibril pattern are seen. In addition, the myofibrils lose the linear shape and become wavy and curved (Figure 3, L-N, Table 1).

Interestingly zebrafish *ntl* mutants do not form a proper notochord, yet do form somites. However, these structures do not demonstrate the classic chevron shaped somite pattern (Halpern et al., 1993). Our *ntl* defect is not a genetic mutation, so there was no complete loss of *ntl* from early embryonic stages. It is interesting that we saw changes in F59 staining at 72hpf and only after the changes are noted in the notochord *ntl* staining at 48hr.

3.3 Vascular Changes in somatic tissue

To investigate if the somitic changes we noticed also resulted in changes in the vasculature pattern within the somitic tissue, we utilized the *fli-1 gfp* transgenic embryos. The *fli-1* promoter drives expression of green fluorescent protein in endothelial blood vessels during development (Lawson and Weinstein, 2002). The signal was weak at 24hrs as the vasculature is developing, but by 48hpf, the GFP signal was strongly expressed in the intersegmental vessels (ISV) and the dorsal aorta. Thus, only the 48 and 72hr time points were examined.

No changes were seen at 48hpf in control or lead exposed embryos looking at gross vascularization or in magnified views of the somatic region (Figure 4 A-D). The intersegmental

ACCEPTED MANUSCRIPT

vessels (ISV) are well developed and extend up from the dorsal aorta (DA). However, by 72hpf, noticeable changes in the vascularization became apparent (Figure 4, E-P). A variety of vascular changes were noted, including incomplete ISVs (Figure 4, H-J), a lack of ISVs (Figure 4, K), abnormal branching patterns of ISVs (Figure 4, L-N), irregularly spaced ISVs (Figure 4, P) and irregularly shaped ISVs (Figure 4, O) (Table 2). Many lead treated embryos demonstrated multiple ISV phenotypes within a single embryo (Table 2).

There is a wealth of literature on blood lead levels as it relates to child health and development, but limited publications on physical alterations to the blood vessels themselves during development in response to lead. Recently, Roy et al., (2014) investigated alterations in blood vasculature in the developing brain in response to lead and found alterations in the central artery of the hindbrain by 72hpf. Vasculature at earlier stages appeared normal (Roy et al., 2014). This was consistent with results presented here in the body. No changes in vasculature were seen prior to 72hpf.

3.4 Neural changes in body

In all vertebrate species, the notochord is required for neurectodermal patterning and signals formation of the floor plate of the neural tube. Additionally, the notochord independently signals formation of motor neurons (Placzek et al., 1991; Stemple et al., 1996; van Straaten and Hekking, 1991; Yamada et al., 1991). Given the *ntl* phenotype we saw (Figure 3), we sought to investigate if lead would alter motor neuron development utilizing two transgenics, *islet-1 gfp* (Higashijima et al., 2000) and *neurogenin1 gfp* (Blader et al., 2003; Fan et al., 2011).

Control and lead treated *islet-1 gfp* embryos developed Rohon-Beard sensory neurons along the length of the anterioposterior (A-P) spine by 48hrs (Figure 5, A-D). Dorsal projections

ACCEPTED MANUSCRIPT

of the spinal motor neurons have not yet extended at 48hrs. By 72hpf, control embryos demonstrated very strong Rohon-Beard neurons along the A-P axis of the spine and show strong dorsally projecting motor neurons (Figure 5, E,F). Lead treated *islet-1 gfp* embryos showed a loss of Rohon-Beard neurons in the anterior spinal region, and weakened and/or jumbled Rohon-Beard cell bodies in the posterior spine (Figure 5, G-J). This is interesting as we also saw a loss of *ntl* expression in the anterior region of the notochord at 48hpf (Figure 3, D). Furthermore, lead treated embryos showed a complete lack of dorsally projecting motor neurons or demonstrated incomplete or abnormal extension of motor neurons (Figure 5, H,J) (Table 3).

The GFP signal in *neurogenin1* transgenic embryos does not become strong until after 48hpf and thus, only the 72hpf time point was assessed. In control embryos, *neurogenin1* was expressed strongly along the length of the entire neural tube (Figure 6 A,C). Dorsal root ganglion (DRG) cells are clearly seen and evenly spaced along the length of the spinal cord (Figure 6, C, D) by 72hpf. Spinal cord motor neurons have extended ventrally to innervate the body tissue (Figure 6, B). By 72hpf, lead treated embryos demonstrated weakened, absent, or incomplete ventral motor neuron extension (Figure 6, E,F,I,J). The evenly spaced pattern of the DRG along the spine became disorganized and unclear (Figure 6, G,H,K,L) (Table 3). In some cases, it became difficult to define the DRG cell bodies.

Studies have shown that ablation of the notochord prevents differentiation of spinal motoneurons (van Straaten and Hekking, 1991; Yamada et al., 1991). Although we did not ablate the notochord, we did detect changes in *ntl* expression in response to lead, suggesting alteration to the notochord structure. This could then alter signals being sent to the neural tube and the signals being sent for development of the spinal motoneurons. This seems consistent with our results in the *islet-1* and *neurogenin1* transgenic embryos. It is interesting however, that

Accepted Manuscript

ACCEPTED MANUSCRIPT

the *neurogenin1* phenotype is consistent along the A-P axis whereas the *islet-1* phenotype appears prominently along the anterior spinal region. Previously, *neurogenin1 (ngn1) in situ* hybridizations have been performed, but only slight changes in *ngn1* expression were found (Dou and Zhang, 2011). However, the only time point assessed in the study was 24hrs. As our transgenic does not produce a strong signal until 72hrs, the earlier time points could not be assessed.

The results seen in regards to motor neurons are interesting and could be correlated with the behavioral and swimming deficits previously noted in the literature. We detected alterations to the Rohon-Beard sensory neurons in the *islet-1* transgenic fish as well as abnormally patterned dorsal root ganglion sensory neurons in the *neurogenin1* transgenic embryos in lead treatments. Furthermore, we detected alterations and/or loss of the dorsally and ventrally extending motor neurons. The changes we detected could be related to known behavioral defects seen in zebrafish including decreases in startle response (Rice et al., 2011), swimming patterns and speeds (Chen et al., 2012; Rice et al., 2011) and escape reactions (Dou and Zhang, 2011).

3.5 Increased Apoptosis

Lastly, we also investigated if lead treatment caused an increase in apoptosis in the body. Others have noted increased apoptosis in response to lead in the brain (Dou and Zhang, 2011; Peterson et al., 2013; Roy et al., 2014), but we also wanted to investigate if the body demonstrated increased levels of apoptosis as well. Control and lead exposed embryos were treated with Acridine Orange live dye staining to detect apoptotic cells at 24, 48 and 72hpf. At 24hr and 48hrs, no gross detectable apoptotic cells were detected in control or lead treated embryos (Figure 7, A-D). At 24hpf, it is common to see some sporadic spots as the embryo has just undergone numerous normal patterning processes including programmed cell death (Figure

ACCEPTED MANUSCRIPT

7, A,B). By 72hpf apoptotic cell clusters became apparent within the somatic tissue (Figure 7, E-H). Some apoptotic cells were sporadic (Figure 7, F) but mainly apoptosis was found in clusters in the notochord and the somites (Figure 7, G,H). Interestingly, the clusters did not necessarily overlap with regions where we noted changes, for example, the anterior spinal regions where *islet-1* motor neurons were lost. This apoptosis could reflect general toxicity of lead at the later time point. The thickness of the body tissue and the limitations of a non-confocal microscope permit only a qualitative assessment of apoptosis.

4. Conclusion

Here, we utilized the well-established zebrafish model of vertebrate developmental toxicity to investigate the effects of lead exposure on the developing body. We provide evidence that lead causes alterations to the notochord and somite morphology using live and *in situ* approaches. Furthermore, we demonstrate lead causes alteration to the body vasculature, changes in Rohon-Beard and dorsal root ganglion sensory neurons, and defects in extension of dorsal and ventrally projecting motor neurons. Increased apoptotic clusters were also noted. These results are interesting and preliminary and in no way demonstrate a mechanism, but a potential interesting connection between early effects of lead on the developing notochord and later staged motor neuron development could be postulated. Future experiments would involve a more comprehensive study of the notochord during lead exposure utilizing other notochord markers like *floating head (flh), momo (mom)* and *doc* required for early notochord development (Odenthal et al., 1996). Additionally, since alterations of *ntl* expression has been shown to alter somatic development, a more comprehensive study of muscle development could be performed looking at other muscle markers like *myf5* and *myogenin* (Weinberg et al., 1996) as well as specific antibody stains to assess changes on fast and slow muscle subtypes. Clearly, much still

Accepted Manuscript

ACCEPTED MANUSCRIPT

remains to be investigated on the developmental toxicity of lead, but here we show lead is developmentally toxic to other aspects of the embryo, not just the brain.

Acknowledgements

The authors wish to thank the Lawson Lab (University of Massachusetts Medical Center) for the *fli-1* transgenic fish, the Linney Lab (Duke University Medical Center) for the *islet-1* and *neurogenin1* transgenic fish, the Devoto Lab (Wesleyan University) and the Barresi Lab (Smith College) for assistance with immunohistochemistries and antibodies. Additionally, we wish to thank Dr. Christopher Lassiter for critically reading the manuscript.

References

Barresi, M. J., D'Angelo, J. A., Hernandez, L. P., and Devoto, S. H. (2001). Distinct mechanisms regulate slow-muscle development. *Curr Biol* **11**(18), 1432-8.

Blader, P., Plessy, C., and Strahle, U. (2003). Multiple regulatory elements with spatially and temporally distinct activities control neurogenin1 expression in primary neurons of the zebrafish embryo. *Mech Dev* **120**(2), 211-8.

Busquet, F., Nagel, R., von Landenberg, F., Mueller, S. O., Huebler, N., and Broschard, T. H. (2008). Development of a new screening assay to identify proteratogenic substances using zebrafish danio rerio embryo combined with an exogenous mammalian metabolic activation system (mDarT). *Toxicol Sci* **104**(1), 177-88.

Chen, J., Chen, Y., Liu, W., Bai, C., Liu, X., Liu, K., Li, R., Zhu, J. H., and Huang, C. (2012). Developmental lead acetate exposure induces embryonic toxicity and memory deficit in adult zebrafish. *Neurotoxicol Teratol* **34**(6), 581-6.

Dai, Y. J., Jia, Y. F., Chen, N., Bian, W. P., Li, Q. K., Ma, Y. B., Chen, Y. L., and Pei, D. S. (2014). Zebrafish as a model system to study toxicology. *Environ Toxicol Chem* **33**(1), 11-7.

Dapul, H., and Laraque, D. (2014). Lead Poisoning in Children. *Adv Pediatr* **61**(1), 313-333.

Devoto, S. H., Melancon, E., Eisen, J. S., and Westerfield, M. (1996). Identification of separate slow and fast muscle precursor cells in vivo, prior to somite formation. *Development* **122**(11), 3371-80.

Dou, C., and Zhang, J. (2011). Effects of lead on neurogenesis during zebrafish embryonic brain development. *J Hazard Mater* **194**, 277-82.

Fan, C. Y., Simmons, S. O., Law, S. H., Jensen, K., Cowden, J., Hinton, D., Padilla, S., and Ramabhadran, R. (2011). Generation and characterization of neurogenin1-GFP transgenic medaka with potential for rapid developmental neurotoxicity screening. *Aquat Toxicol* **105**(1-2), 127-35.

ACCEPTED MANUSCRIPT

Goldstone, J. V., McArthur, A. G., Kubota, A., Zanette, J., Parente, T., Jonsson, M. E., Nelson, D. R., and Stegeman, J. J. (2010). Identification and developmental expression of the full complement of Cytochrome P450 genes in Zebrafish. *BMC Genomics* **11**, 643.
Grunwald, D. J., and Eisen, J. S. (2002). Headwaters of the zebrafish -- emergence of a new model vertebrate. *Nat Rev Genet* **3**(9), 717-24.
Halpern, M. E., Ho, R. K., Walker, C., and Kimmel, C. B. (1993). Induction of muscle pioneers and floor plate is distinguished by the zebrafish no tail mutation. *Cell* **75**(1), 99-111.
Hernberg, S. (2000). Lead poisoning in a historical perspective. *Am J Ind Med* **38**(3), 244-54.
Higashijima, S., Hotta, Y., and Okamoto, H. (2000). Visualization of cranial motor neurons in live transgenic zebrafish expressing green fluorescent protein under the control of the islet-1 promoter/enhancer. *J Neurosci* **20**(1), 206-18.
Hill, A. J., Teraoka, H., Heideman, W., and Peterson, R. E. (2005). Zebrafish as a model vertebrate for investigating chemical toxicity. *Toxicol Sci* **86**(1), 6-19.
Howe, K., Clark, M. D., Torroja, C. F., Torrance, J., Berthelot, C., Muffato, M., Collins, J. E., Humphray, S., McLaren, K., Matthews, L., McLaren, S., Sealy, I., Caccamo, M., Churcher, C., Scott, C., Barrett, J. C., Koch, R., Rauch, G. J., White, S., Chow, W., Kilian, B., Quintais, L. T., Guerra-Assuncao, J. A., Zhou, Y., Gu, Y., Yen, J., Vogel, J. H., Eyre, T., Redmond, S., Banerjee, R., Chi, J., Fu, B., Langley, E., Maguire, S. F., Laird, G. K., Lloyd, D., Kenyon, E., Donaldson, S., Sehra, H., Almeida-King, J., Loveland, J., Trevanion, S., Jones, M., Quail, M., Willey, D., Hunt, A., Burton, J., Sims, S., McLay, K., Plumb, B., Davis, J., Clee, C., Oliver, K., Clark, R., Riddle, C., Elliot, D., Threadgold, G., Harden, G., Ware, D., Begum, S., Mortimore, B., Kerry, G., Heath, P., Phillimore, B., Tracey, A., Corby, N., Dunn, M., Johnson, C., Wood, J., Clark, S., Pelan, S., Griffiths, G., Smith, M., Glithero, R., Howden, P., Barker, N., Lloyd, C., Stevens, C., Harley, J., Holt, K., Panagiotidis, G., Lovell, J., Beasley, H., Henderson, C., Gordon, D., Auger, K., Wright, D., Collins, J., Raisen, C., Dyer, L., Leung, K., Robertson, L., Ambridge, K., Leongamornlert, D., McGuire, S., Gilderthorp, R., Griffiths, C., Manthravadi, D., Nichol, S., Barker, G., Whitehead, S., Kay, M., Brown, J., Murnane, C., Gray, E., Humphries, M., Sycamore, N., Barker, D., Saunders, D., Wallis, J., Babbage, A., Hammond, S., Mashreghi-Mohammadi, M., Barr, L., Martin, S., Wray, P., Ellington, A., Matthews, N., Ellwood, M., Woodmansey, R., Clark, G., Cooper, J., Tromans, A., Grafham, D., Skuce, C., Pandian, R., Andrews, R., Harrison, E., Kimberley, A., Garnett, J., Fosker, N., Hall, R., Garner, P., Kelly, D., Bird, C., Palmer, S., Gehring, I., Berger, A., Dooley, C. M., Ersan-Urun, Z., Eser, C., Geiger, H., Geisler, M., Karotki, L., Kirn, A., Konantz, J., Konantz, M., Oberlander, M., Rudolph-Geiger, S., Teucke, M., Lanz, C., Raddatz, G., Osoegawa, K., Zhu, B., Rapp, A., Widaa, S., Langford, C., Yang, F., Schuster, S. C., Carter, N. P., Harrow, J., Ning, Z., Herrero, J., Searle, S. M., Enright, A., Geisler, R., Plasterk, R. H., Lee, C., Westerfield, M., de Jong, P. J., Zon, L. I., Postlethwait, J. H., Nusslein-Volhard, C., Hubbard, T. J., Roest Crollius, H., Rogers, J., and Stemple, D. L. (2013). The zebrafish reference genome sequence and its relationship to the human genome. *Nature* **496**(7446), 498-503.
Kimmel, C. B., Ballard, W. W., Kimmel, S. R., Ullmann, B., and Schilling, T. F. (1995). Stages of embryonic development of the zebrafish. *Dev Dyn* **203**(3), 253-310.
Lawson, N. D., and Weinstein, B. M. (2002). In vivo imaging of embryonic vascular development using transgenic zebrafish. *Dev Biol* **248**(2), 307-18.
Lidsky, T. I., and Schneider, J. S. (2003). Lead neurotoxicity in children: basic mechanisms and clinical correlates. *Brain* **126**(Pt 1), 5-19.
Needleman, H. (2004). Lead poisoning. *Annu Rev Med* **55**, 209-22.
Odenthal, J., Haffter, P., Vogelsang, E., Brand, M., van Eeden, F. J., Furutani-Seiki, M., Granato, M., Hammerschmidt, M., Heisenberg, C. P., Jiang, Y. J., Kane, D. A., Kelsh, R. N., Mullins, M. C., Warga, R. M., Allende, M. L., Weinberg, E. S., and Nusslein-Volhard, C. (1996). Mutations affecting the formation of the notochord in the zebrafish, Danio rerio. *Development* **123**, 103-15.

ACCEPTED MANUSCRIPT

Padilla, S., Corum, D., Padnos, B., Hunter, D. L., Beam, A., Houck, K. A., Sipes, N., Kleinstreuer, N., Knudsen, T., Dix, D. J., and Reif, D. M. (2012). Zebrafish developmental screening of the ToxCast Phase I chemical library. *Reprod Toxicol* **33**(2), 174-87.
Peterson, S. M., Zhang, J., and Freeman, J. L. (2013). Developmental reelin expression and time point-specific alterations from lead exposure in zebrafish. *Neurotoxicol Teratol* **38**, 53-60.
Philp, R. B. (2001). *Ecosystems and human health : toxicology and environmental hazards*. 2nd ed. Lewis Publishers, Boca Raton.
Placzek, M., Yamada, T., Tessier-Lavigne, M., Jessell, T., and Dodd, J. (1991). Control of dorsoventral pattern in vertebrate neural development: induction and polarizing properties of the floor plate. *Development* **Suppl 2**, 105-22.
Rice, C., Ghorai, J. K., Zalewski, K., and Weber, D. N. (2011). Developmental lead exposure causes startle response deficits in zebrafish. *Aquat Toxicol* **105**(3-4), 600-8.
Roy, N. M., DeWolf, S., Schutt, A., Wright, A., and Steele, L. (2014). Neural alterations from lead exposure in zebrafish. *Neurotoxicol Teratol* **46C**, 40-48.
Sagerstrom, C. G., Grinbalt, Y., and Sive, H. (1996). Anteroposterior patterning in the zebrafish, Danio rerio: an explant assay reveals inductive and suppressive cell interactions. *Development* **122**(6), 1873-83.
Schulte-Merker, S., Hammerschmidt, M., Beuchle, D., Cho, K. W., De Robertis, E. M., and Nusslein-Volhard, C. (1994). Expression of zebrafish goosecoid and no tail gene products in wild-type and mutant no tail embryos. *Development* **120**(4), 843-52.
Selderslaghs, I. W., Van Rompay, A. R., De Coen, W., and Witters, H. E. (2009). Development of a screening assay to identify teratogenic and embryotoxic chemicals using the zebrafish embryo. *Reprod Toxicol* **28**(3), 308-20.
Stemple, D. L., Solnica-Krezel, L., Zwartkruis, F., Neuhauss, S. C., Schier, A. F., Malicki, J., Stainier, D. Y., Abdelilah, S., Rangini, Z., Mountcastle-Shah, E., and Driever, W. (1996). Mutations affecting development of the notochord in zebrafish. *Development* **123**, 117-28.
Tao, T., and Peng, J. (2009). Liver development in zebrafish (Danio rerio). *J Genet Genomics* **36**(6), 325-34.
Teraoka, H., Dong, W., and Hiraga, T. (2003). Zebrafish as a novel experimental model for developmental toxicology. *Congenit Anom (Kyoto)* **43**(2), 123-32.
Tong, S., von Schirnding, Y. E., and Prapamontol, T. (2000). Environmental lead exposure: a public health problem of global dimensions. *Bull World Health Organ* **78**(9), 1068-77.
van Straaten, H. W., and Hekking, J. W. (1991). Development of floor plate, neurons and axonal outgrowth pattern in the early spinal cord of the notochord-deficient chick embryo. *Anat Embryol (Berl)* **184**(1), 55-63.
Virta, V. C., and Cooper, M. S. (2011). Structural components and morphogenetic mechanics of the zebrafish yolk extension, a developmental module. *J Exp Zool B Mol Dev Evol* **316**(1), 76-92.
Weinberg, E. S., Allende, M. L., Kelly, C. S., Abdelhamid, A., Murakami, T., Andermann, P., Doerre, O. G., Grunwald, D. J., and Riggleman, B. (1996). Developmental regulation of zebrafish MyoD in wild-type, no tail and spadetail embryos. *Development* **122**(1), 271-80.
Westerfield, M. (1993). *The zebrafish book : a guide for the laboratory use of zebrafish (Brachydanio rerio)*. M. Westerfield, Eugene, OR.
Yamada, T., Placzek, M., Tanaka, H., Dodd, J., and Jessell, T. M. (1991). Control of cell pattern in the developing nervous system: polarizing activity of the floor plate and notochord. *Cell* **64**(3), 635-47.

Figures

ACCEPTED MANUSCRIPT

Figure 1: Live images of control and lead treated embryos. (A-D), 24hpf, (E-H), 48hpf, (I-L), 72hpf. Control (A,B,E,F,I,J) and lead treated (C,D,G,H,K,L). All images are lateral views, anterior to left. Images are shown in full view (A,C,E,G,I,K) next to magnified view of the somatic tissue (B,D,F,H,J,L). Dashed lines represent somite boundaries. Double arrow represents the notochord width. Arrows (L) represent altered and unclear somatic boundaries. YSE: Yolk sac extension.

Figure 2: Somite measurements at 24, 48 and 72hpf. Measurements are in millimeters. Each value represents means +/- standard deviations of a total of 30 embryos (three independent experiments with an n of 10 each for control and lead were performed). Asterisk denotes lead treatment value of less than 0.05.

Figure 3: *In situ* hybridization and immunohistochemistry at 24, 48 and 72hpf. (A,B,G,H) 24hpf, (C,D,I,J) 48hpf, (E,F,K-N) 72hpf. Control (A,C,E,G,I,K) and lead treated (B,D,F,H,J,L,M,N). All images are lateral views, anterior to left. (A-F) *ntl in situ* staining with magnified inset, (G-N) F59 antibody staining. Dashed lines represent somite boundaries. Arrows denote gaps in the myofibril pattern within the somite and arrowheads denote non-linear wavy myofibrils.

Table 1: Total number of embryos in control and lead treatments demonstrating wild-type and aberrant phenotypes for *ntl in situ* hybridization and F59 antibody staining at 24, 48 and 72hpf. Numbers are shown as fractions and percentages. A total of 30 embryos per treatment were tested (three independent experiments with an n of 10 each for control and lead were performed).

Figure 4: Somitic vasculature visualized with *fli-1 gfp* transgenics. (A-D) 48hpf, (E-P) 72hpf. Control (A,B,E,F) and lead treated (C,D,G-P). All images are lateral views, anterior to left.

ACCEPTED MANUSCRIPT

Images are shown in full view (A,C,E,G) or in magnified views to illustrate vascular changes (B,D,F,H-P) shown by arrows. ISV: intersegmental vesicle, DA: dorsal aorta.

Table 2: Total number of embryos in control and lead treatments demonstrating aberrant phenotypes at 48 and 72hpf in *fli-1 gfp* transgenic embryos. Numbers are shown as fractions and percentages. A total of 30 embryos per treatment were tested (three independent experiments with an n of 10 each for control and lead were performed).

Figure 5: Neuron development in the body utilizing *islet-1 gfp* transgenic embryos. (A-D) 48hpf, (E-J) 72hpf. (A,B,E,F) control and (C,D,G-J) lead treated. All images are lateral views, anterior to left. Images are shown in full view (A,C,E,G,I) next to magnified view of the somatic tissue (B,D,F,H,J). Dashed lines represent somite boundaries. RB: Rohon-Beard neurons, arrowheads denote dorsal extension of motor neurons from spinal cord.

Figure 6: Neuron development in the body utilizing *neurogenin1 gfp* transgenic embryos. (A-L) 72hpf. (A-D) control and (E-L) lead treated. (A,B,E,F,I,J) lateral views, anterior to left, (C,D,G,H,K,L) dorsal views, anterior to left. Images are shown in full view (A,C,E,G,I,K) next to magnified view of the somatic tissue (B,D,F,H,J,L). DRG: Dorsal root ganglion, arrowheads denote ventral extension of motor neurons from spinal cord, asterisks denotes incomplete or missing motor neuron extension.

Table 3: Total number of embryos in control and lead treatments demonstrating aberrant phenotypes at 48 and 72hpf for *islet-1 gfp* and *neurogenin1 gfp* transgenics. Numbers are shown as fractions and percentages. A total of 30 embryos per treatment were tested (three independent experiments with an n of 10 each for control and lead were performed).

Accepted Manuscript

ACCEPTED MANUSCRIPT

Figure 7: Apoptosis in the somatic tissue. (A,B) 24hpf, (C,D) 48hpf, (E-H) 72hpf. (A,C,E) control and (B,D,F-H) lead treated in lateral views. Control somitic tissue demonstrated few apoptotic spots (A,C,E) at 24,48 or 72hpf. Lead treated embryos showed few apoptotic spots at 24 or 48hpf (B,D), but demonstrate increased numbers of apoptotic cells (F) or large apoptotic cellular clusters (G,H) by 72hpf. Dashed lines outline somatic boundaries, arrows note apoptotic clusters.

Accepted Manuscript

ACCEPTED MANUSCRIPT

ntl				
Time	*Treatment*	*Normal expression along A-P axis*	*Weakened anterior spine expression*	*Overall weakened expression along A-P axis*
24hr	Control	30/30 (100%)	0/30 (0%)	0/30 (0%)
	Lead	30/30 (100%)	0/30 (0%)	0/30 (0%)
48hr	Control	29/30 (96.6%)	1/30 (3.3%)	0/30 (0%)
	Lead	5/30 (16.6%)	25/30 (83.3%)	0/30 (0%)
72hr	Control	30/30 (100%)	0/30 (0%)	0/30 (0%)
	Lead	0/30 (0%)	12/30 (40%)	18/30 (60%)
n=10 per experiment, replicate=3				
F59 Antibody				
Time	*Treatment*	*Normal chevron shaped expression within somite*	*Gaps within myofibrils*	*Non-linear myofibrils (curvy myofibrils)*
24hr	Control	30/30 (100%)	0/30 (0%)	0/30 (0%)
	Lead	30/30 (100%)	0/30 (0%)	0/30 (0%)
48hr	Control	30/30 (100%)	0/30 (0%)	0/30 (0%)
	Lead	27/30 (90%)	1/30 (3.3%)	0/30 (0%)
72hr	Control	30/30 (100%)	0/30 (0%)	0/30 (0%)
	Lead	6/30 (20%)	22/30 (73.3%)	26/30 (86.7%)
n=10 per experiment, replicate=3				

Table 1

Accepted Manuscript

ACCEPTED MANUSCRIPT

fli-1						
Time	*Treatment*	*lack of ISV*	*incomplete ISV*	*branching of ISV*	*irregular spacing of ISV*	*irregular shaped ISV*
48hr	Control	0/30 (0%)	1/30 (3.3%)	2/30 (6.7%)	0/30 (0%)	1/30 (3.3%)
	Lead	0/30 (0%)	2/30 (6.6%)	3/30 (10%)	0/30 (0%)	2/30 (6.6%)
72hr	Control	0/30 (0%)	2/30 (6.7%)	2/30 (6.7%)	0/30 (0%)	2/30 (6.7%)
	Lead	10/30 (33.3%)	19/30 (63.3%)	17/30 (56.7%)	23/30 (76.7%)	21/30 (70%)
n=10 per experiment, replicate=3						

Table 2

Accepted Manuscript

ACCEPTED MANUSCRIPT

islet-1gfp					
Time	*Treatment*	*lack of motor neuron dorsal extension*	*incomplete/abnormal extension of motor neuron dorsal extension*	*Rohon-Beard cells fully present along A-P axis*	*Rohon-Beard cells incomplete along A-P axis*
48hr	Control	30/30 (100%)	0/30 (0%)	28/30 (93.3%)	2/30 (6.6%)
	Lead	30/30 (100%)	0/30 (0%)	27/30 (90%)	3/30 (10%)
72hr	Control	0/30 (0%)	0/30 (0%)	30/30 (100%)	0/30 (0%)
	Lead	12/30 (40%)	18/30 (60%)	3/30 (10%)	27/30 (90%)
n=10 per experiment, replicate=3					

neurogenin1 gfp					
Time	*Treatment*	*lack of motor neuron ventral extension*	*incomplete/abnormal extension of motor neuron ventral extension*	*Dorsal root ganglion cells fully present and evenly spaced along A-P axis*	*Dorsal root ganglion cells absent/altered along A-P axis*
72hr	Control	0/30 (0%)	0/30 (0%)	30/30 (100%)	0/30 (0%)
	Lead	2/30 (6.6%)	28/30 (93.3%)	3/30 (10%)	27/30 (90%)
n=10 per experiment, replicate=3					

Accepted Manuscript

ACCEPTED MANUSCRIPT

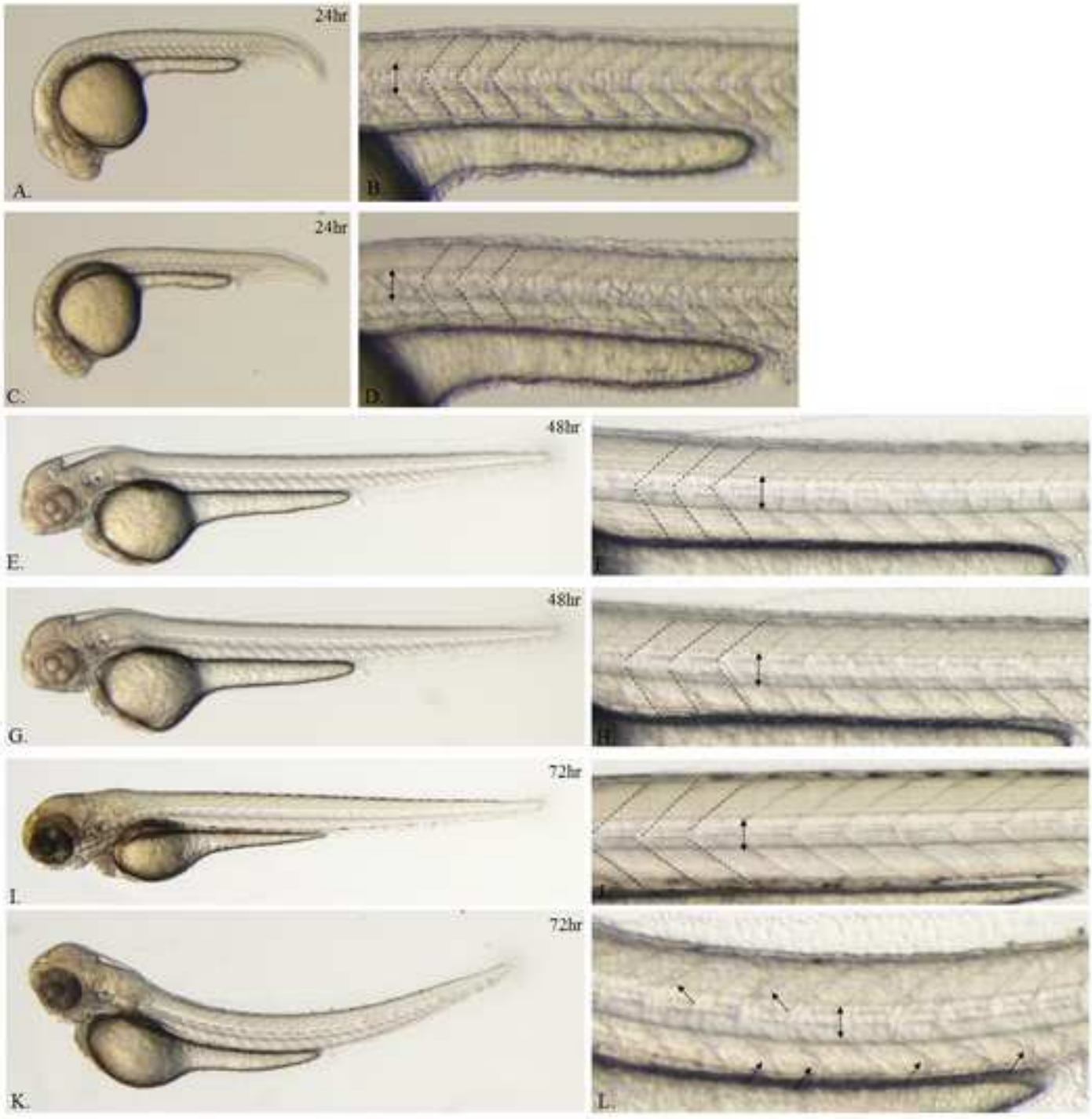

ACCEPTED MANUSCRIPT

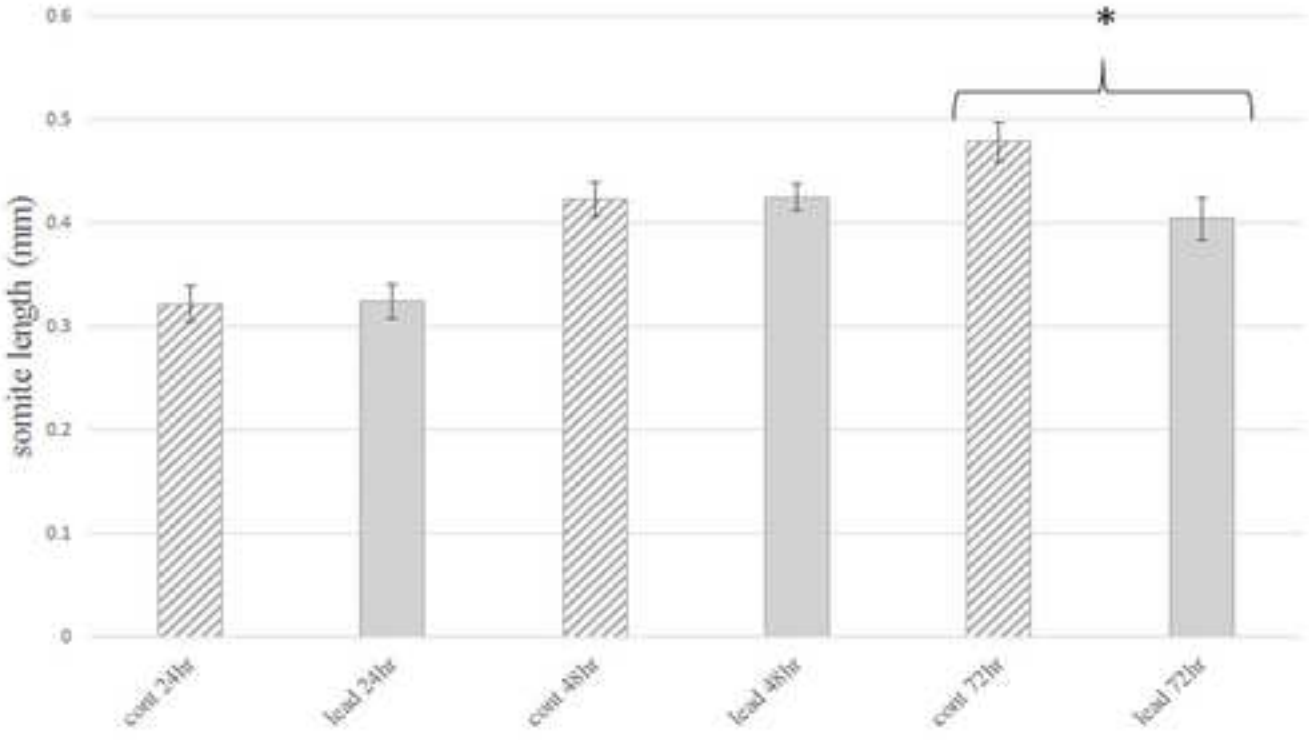

ACCEPTED MANUSCRIPT

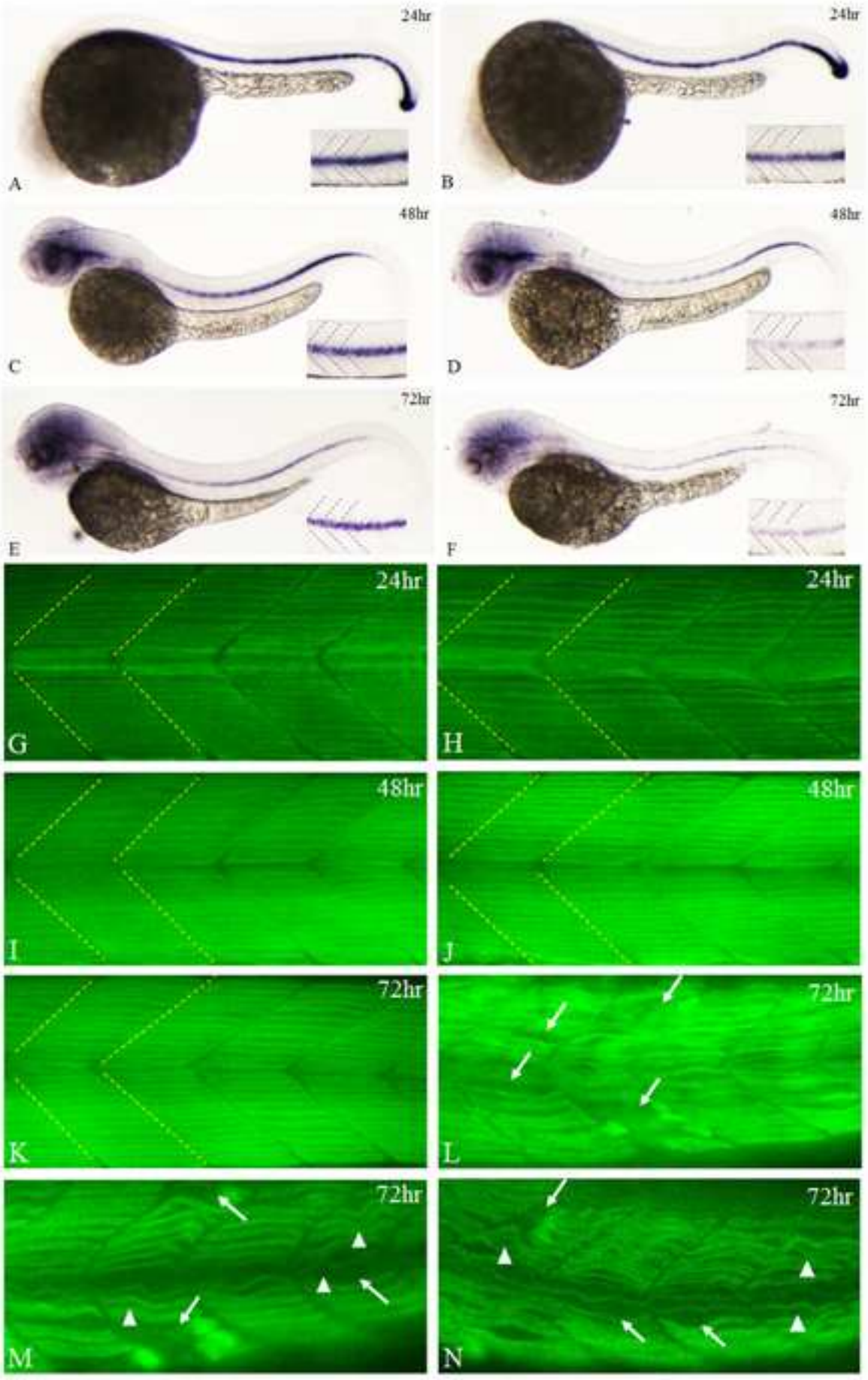

ACCEPTED MANUSCRIPT

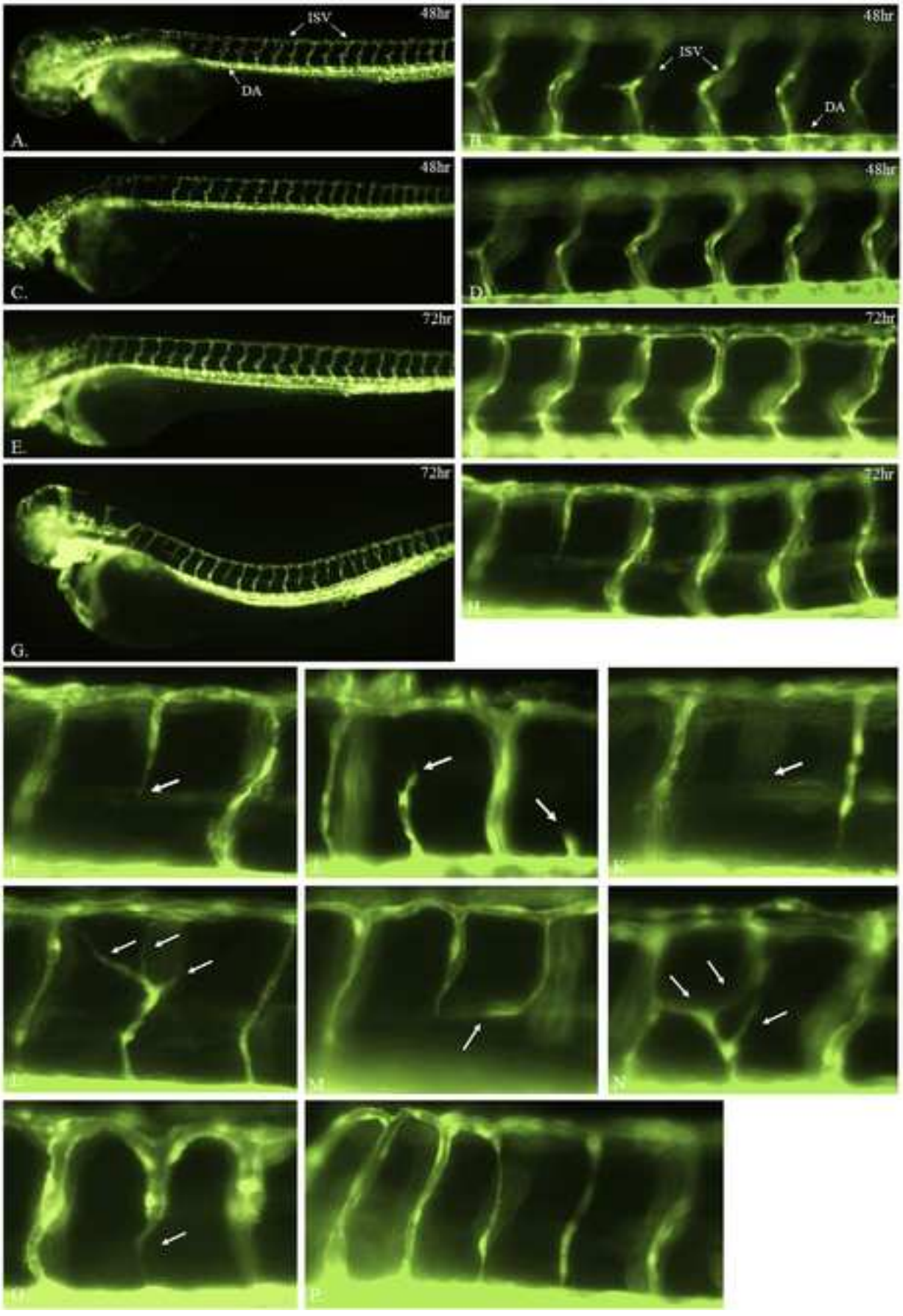

ACCEPTED MANUSCRIPT

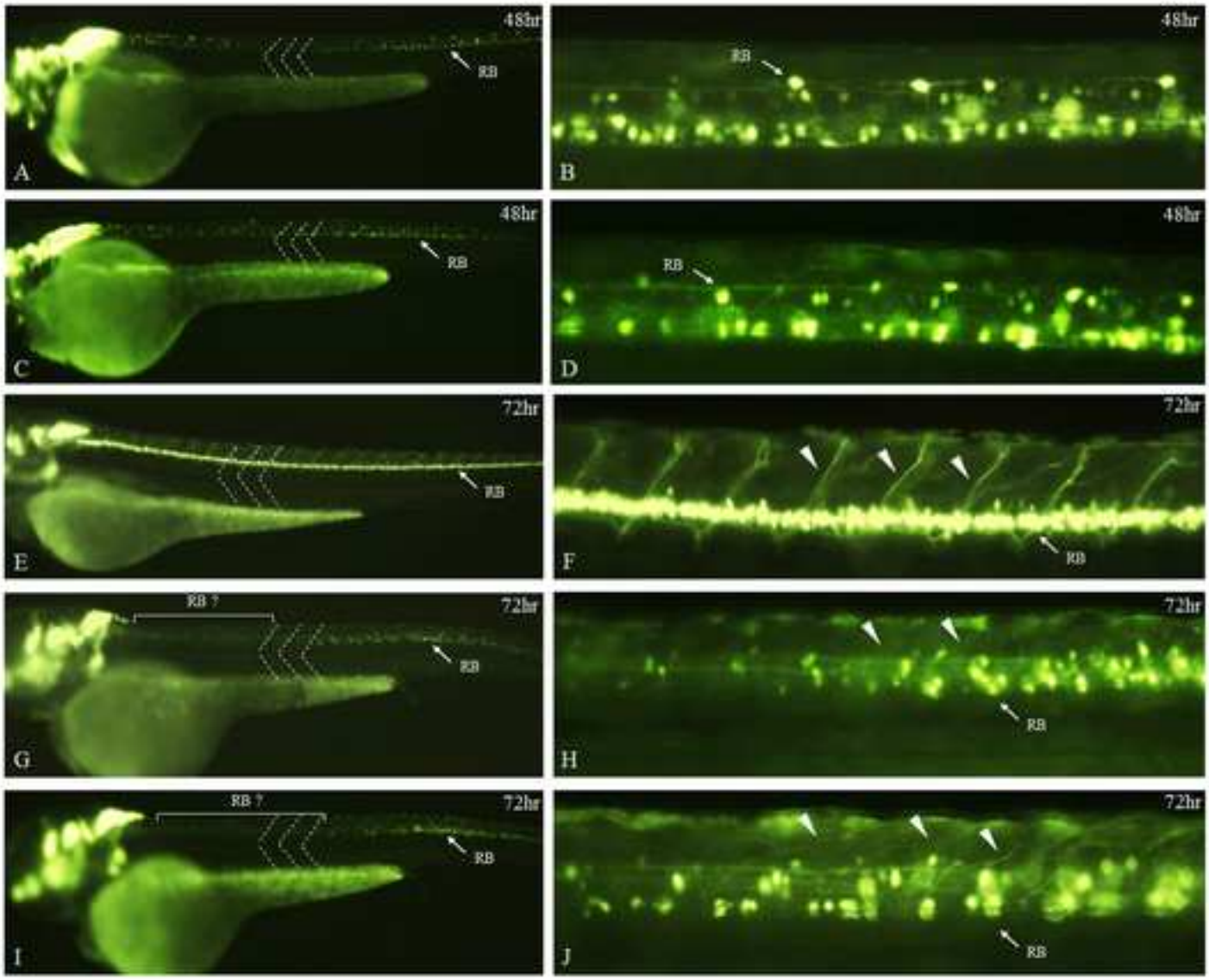

ACCEPTED MANUSCRIPT

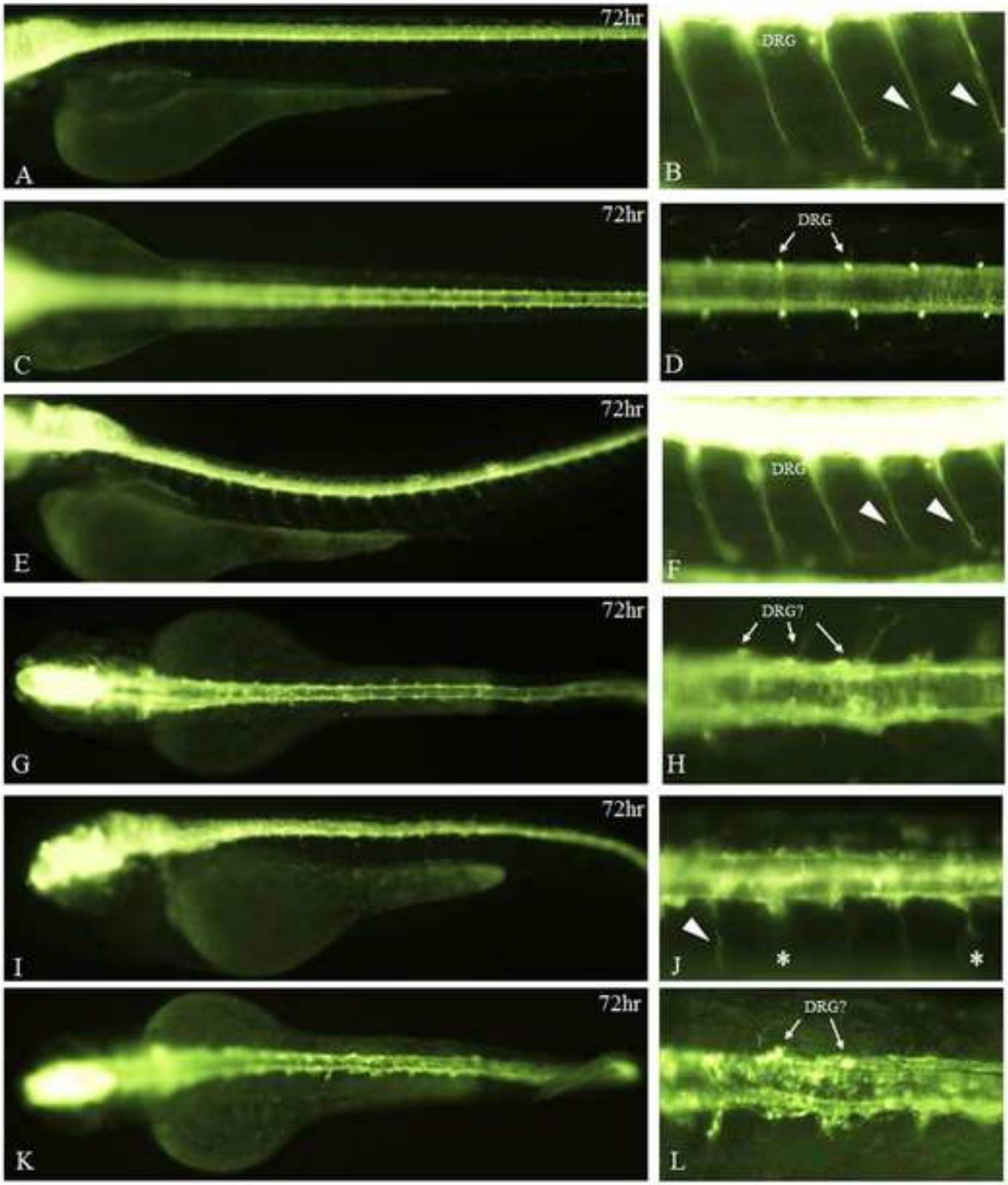

ACCEPTED MANUSCRIPT